Automotive Experiences
Vol. 8 No. 2 (2025) pp. 390-400
p-ISSN: 2615-6202 e-ISSN: 2615-6636

Research Paper

Development and Evaluation of Passive Balancing System Model for Lithium-Ion Battery Pack in Electric Vehicles using Numerical Simulation

Vu Hai Quan[1], **Karpukhin Kirill Evgenievich**[2], **Nguyen Trong Duc**[3], **Karpukhin Filipp Kirillovich**[4]

[1]School of Mechanical Automotive Engineering, Hanoi University of Industry, Hanoi 100000, Vietnam
[2]Federal State Unitary Enterprise "Central Scientific Research Automobile and Automotive Engines Institute" (FSUE "NAMI"), Moscow 125438, Russia Federation
[3]Moscow Automobile and Road Construction State Technical University (MADI), Moscow 125319, Russia Federation
[14]Moscow Polytechnic University, Moscow 107023, Russian Federation

quanvh@haui.edu.vn

https://doi.org/10.31603/ae.13320

Published by Automotive Laboratory of Universitas Muhammadiyah Magelang

Article Info
Submitted:
15/03/2025
Revised:
13/09/2025
Accepted:
13/09/2025
Online first:
25/09/2025

Abstract

Electric vehicles (EVs) are increasingly becoming a crucial solution to mitigate environmental pollution and ensure energy security. Batteries, particularly Lithium-ion batteries, are the core component that determines the performance, range, and durability of EVs. However, managing and balancing the state of charge (SOC) among hundreds of cells in a battery pack is a significant challenge due to its complexity and high accuracy requirements. This study addresses these gaps by developing an integrated electro-thermal passive balancing model that combines Thevenin equivalent circuit modeling with dynamic thermal analysis and Stateflow-based MOSFET control logic, specifically designed for EV battery pack applications under realistic urban driving cycles. The passive voltage balancing process is designed to maintain voltage homogeneity among cells, thereby enhancing the pack's efficiency and lifespan. Initial assumptions are made to reduce model complexity (3 Lithium-ion cells), although this may lead to some discrepancies with real-world scenarios. Simulation results show that charging and discharging processes are efficiently managed, with SOC balancing among cells being maintained nearly perfectly after several cycles. Voltage, current, and temperature plots demonstrate stability and uniformity in cell operation thanks to the passive balancing mechanism. However, the current model is limited in reflecting real-world conditions, such as continuous changes in speed and load when the vehicle is in motion. This study provides insights into the operation of EV battery packs through electro-thermal modeling, while suggesting future directions to improve the model's realism and applicability in diverse operating scenarios. The results emphasize the importance of cell balancing in optimizing performance and prolonging the lifespan of EV battery systems.

Keywords: Electric vehicle; Lithium-ion battery; State of charge; Electro-thermal modeling; Passive balancing; Equivalent circuit method

1. Introduction

The resurgence of electric vehicles (EVs) [1], [2], [3] as a cornerstone of sustainable transportation has been driven by advancements in battery technology and growing environmental concerns. Modern EVs rely on lithium-ion (Li-ion) [4], [5] batteries due to their high energy density and efficiency, but their performance is constrained by imbalances in cell state-of-charge (SOC) during operation. Passive balancing methods [6], such as resistor-based networks, remain prevalent in commercial battery management systems (BMS) due to their simplicity. However, these approaches suffer from critical limitations: (1) they fail to account for electro-thermal coupling dynamics during pulsed EV loads, leading to thermal hotspots and accelerated degradation; (2) their static balancing logic results in slow convergence (e.g., >3–5 cycles for <1% SOC deviation); and (3) they are not optimized for dynamic urban driving cycles, where rapid charge-discharge transitions exacerbate cell mismatches.

Existing studies, such as those by Meng *et al*. [7] and Amin *et al*. [8], have advanced passive balancing models for lithium-ion battery packs in electric vehicles (EVs), yet these approaches predominantly rely on simplified electrical equivalent circuit models (ECMs) without integrated thermal feedback. Similarly, Uzair *et al*. [9] provide a comprehensive review of battery management systems (BMS), encompassing architectures, functions, modeling techniques, and both active and passive cell balancing methodologies, with simulations demonstrating the superior efficiency of active balancing over passive techniques for lithium-ion batteries in EVs; however, their analysis still emphasizes ECM-based frameworks lacking real-time thermal integration. Furthermore, most existing approaches utilize static resistor networks with fixed control strategies, limiting their effectiveness under dynamic EV operating conditions characterized by rapid charge-discharge cycles and varying load demands.

The integration of electro-thermal coupling in passive balancing systems remains underexplored, particularly in the context of real-time thermal-voltage interactions during EV-like pulsed loads. Additionally, there is a lack of comprehensive modeling frameworks that can simultaneously simulate electrical dynamics, thermal behavior, and intelligent control logic while maintaining computational efficiency suitable for real-time applications.

The current EV market is diverse, encompassing various segments and manufacturers. Wuling EV stands out in the compact urban EV segment, offering afforda-ble options [10]. VinFast, a Vietnamese manufacturer, has rapidly developed models such as the VF5, focusing on modern design, urban mobility, and investment in charging infrastructure (**Figure 1**). Tesla, a leading U.S. manufacturer, is renowned for its high-performance vehicles, including the Model S, 3, X and Y, as well as ad-vanced technologies like the Supercharger fast-charging network, shaping the premium EV segment and driving technological innovation. This diversity highlights the comprehensive development of the EV market, catering to a wide range of consumer needs.

Batteries are the cornerstone of EVs, determining driving range, performance and sustainability (**Figure 2**). Li-ion battery technology currently dominates due to its high energy density and efficiency, enabling EVs to achieve driving ranges of 320–480 km. However, Li-ion batteries face challenges such as limited energy density, capacity degradation over time and reliance on finite resources like lithium and cobalt. Current research focuses on solid-state batteries (promising higher energy density and safety), Lithium-Sulfur (Li-S) and Lithium-Air batteries (offering potential for superior energy density), and cobalt-free, nickel-rich chemistries (enhancing cost-effectiveness and sustainability). Initiatives in battery recycling and the development of ultra-fast and wireless charging technologies also play a vital role. The future of EV battery technology holds significant promise, with advancements poised to drive widespread EV adoption and shape sustainable transportation.

Lithium-ion and NiMH batteries are the main EV technologies with Li-ion offering high energy density (500+ Wh/kg), efficiency, and longevity but at a higher cost, while NiMH provides a cheaper, durable and recyclable alternative despite lower energy density (60–120 Wh/kg) and memory effect [11], [12], [13], [14].

Figure 1. Battery system and EV charging infrastructure

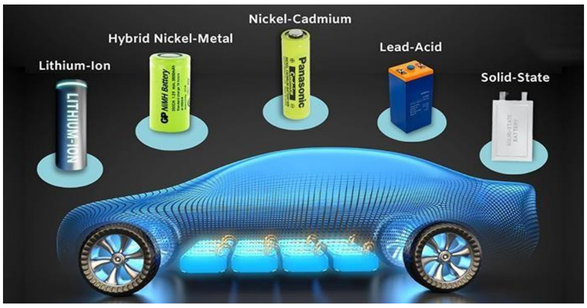

Figure 2. Types of batteries used in electric vehicles

2. Electro-Thermal Modeling of Battery Cells

Figure 3 illustrates the schematic representation of the electro-thermal model developed to predict the electrical and thermal behavior of battery cells. The input current is utilized to calculate the state of charge (SOC), internal resistance and terminal voltage in the electrical model, which is then coupled with the thermal model to determine heat generation and the evolution of cell temperature [15].

In electric vehicles (EVs), determining the state of charge (SOC) and state of health (SOH) of batteries is critical for ensuring safe and efficient operation, as battery energy cannot be directly measured like fossil fuels. Battery models play an essential role in predicting the electrical and thermal behavior of batteries and are categorized into three main groups: empirical models, electrochemical models and equivalent circuit method (ECM).

2.1. Equivalent Circuit Method (ECM)

The ECM approach employs electrical circuit components such as resistors, capacitors and voltage sources to simulate battery behavior, though it does not reflect the physical structure of the cell. ECMs vary in complexity and accuracy, including models such as Thevenin, Rint, Dual Polarization (DP) and those utilizing extended Kalman filters (EKF) [7].

2.1.1. Thevenin Model

The Thevenin model [16] uses a series resistor and parallel RC networks to describe the battery's response to load, assuming a constant open-circuit voltage (OCV). Accuracy improves with the addition of RC networks, with parameters such as polarization resistance (R_1), polarization capacitance (C_1) and RC network voltage (U_t) incorporated into the model equations.

Figure 4 depicts the Thevenin model of a battery, where R_1 is the polarization resistance, C_1 is the polarization capacitance and U_1 is the voltage across the RC network. The model equation is given by Eq. (1).

$$U_t = U_{OC} - U_1 - I.R_0 \tag{1}$$

2.1.2. Rint Model

The Rint model (internal resistance model – Rint) [17], also known as the internal resistance model (Figure 5), is a simple ECM comprising an ideal voltage source (U_{OC}) and an internal resistance (R_0). The output voltage (U_t) is calculated based on the current (I), with parameters varying according to SOC, temperature and current direction (charge/discharge). The governing equation is following Eq. (2).

$$U_t = U_{OC} - I.R_0 \tag{2}$$

where, U_t is the output voltage, (R_0) is the internal resistance, (U_{OC}) represents the open-circuit voltage (OCV, a function of SOC) and (I) is the battery discharge current.

2.1.3. Coulomb Counting (CC)

Coulomb Counting (CC), also known as the Ampere-hour method, is a widely used technique

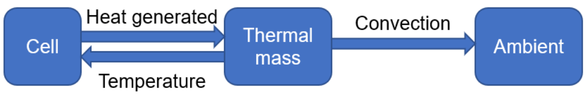

Figure 3. Schematic representation of the electro-thermal model for battery cells

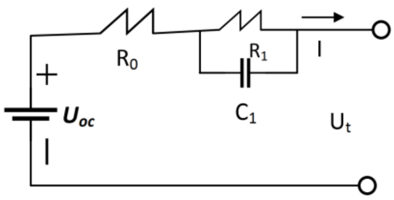

Figure 4. Thevenin model

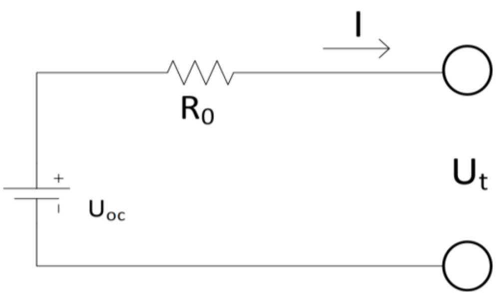

Figure 5. Simple equivalent circuit model

for estimating the state of charge (SOC) and state of health (SOH) of batteries as following Eq. (3) and Eq. (4). This method relies on integrating the current flowing into or out of the battery during charge-discharge cycles, using equations related to initial SOC, rated capacity and battery current [18].

$$SOC(t) = SOC(t_0) - \frac{1}{Q_{rated}} \int_{t_0}^{t} \eta(t) I_{batt} dt \quad (3)$$

$$SOH(t) = \frac{1}{Q_{rated}} \int_{t_0}^{t} I(t) dt \quad (4)$$

where, $SOC(t_0)$ is the initial SOC, Q_{rated} is the rated capacity, I_{batt} is the battery current, and (I) is the discharge current.

The Coulomb Counting method requires accurate initial SOC and precise current measurements but is affected by sensor noise and losses, leading to discrepancies, which studies like Berecibar *et al*. [19] address through OCV-based SOC estimation and periodic calibration for improved accuracy.

2.2. Thermal Modeling

Temperature significantly impacts battery performance, with an optimal operating range of 20–40 °C. Low temperatures reduce capacity due to increased internal resistance, while high temperatures accelerate aging and pose safety risks. Cooling/heating systems are essential to maintain battery performance. The thermodynamic and kinetic properties of chemical reactions within the battery form the basis for thermal modeling [20].

2.2.1. Heat Generation

Heat generation in batteries includes reversible heat (dependent on SOC, which can be exothermic or endothermic) and irreversible heat (always positive). The energy conservation model is used to relate heat generation to temperature evolution, with the following Eq. (5) to Eq. (7) [21].

$$\dot{Q} = \dot{Q_{irr}} + \dot{Q_{rew}} \quad (5)$$

$$\dot{Q} = I(U - OCV) + IT\frac{dU}{dT} \quad (6)$$

$$\frac{d(\rho c_p T)}{dt} = -hA(T - T_c) + \dot{Q} \quad (7)$$

where, ρ is the density, c_p is the specific heat, T and T_c are the cell temperature and the temperature of cooling medium, h is the heat transfer coefficient, A is the cell outer surface area and $\dot{Q}$ is the total heat generated.

3. Simulation Modeling of a Lithium-ion Battery Pack

3.1. Three-Cell Series Battery Pack Model

Electric vehicle (EV) batteries typically consist of hundreds of small cells arranged in series and parallel configurations to achieve the desired voltage and capacity. A typical battery pack comprises modules of 18–30 parallel cells connected in series to meet voltage requirements; for instance, the Tesla Model 3 utilizes over 7,000 lithium-ion cells.

Simulating such a large number of cells poses significant computational challenges, depending on the expertise of the simulation engineer and the capabilities of the simulation hardware. Therefore, in this study, a simplified battery pack consisting of three lithium-ion cells is simulated to reduce complexity (**Figure 6**). The key parameters investigated include state of charge (SOC), current (I), voltage (V), battery temperature and the passive balancing process.

In the simulation model of the three-cell lithium-ion battery pack, the following functional blocks are established:

- Convective heat transfer block: Simulates heat transfer between adjacent cells, representing the temperature exchange among them.
- Perfect insulator block: Represents the third cell, which is not in direct contact with the environment or cooling system, ensuring 393 tis thermally isolated from external influences.
- Temperature sensor block: Measures the temperature of each cell during charge and discharge processes.
- Voltage sensor block: Monitors the voltage of each cell to track operational status.
- Current sensor block: Measures the current intensity of each cell, providing data on current flow during operation. Diode and Load Resistance Block: Consumes electrical energi to facilitate passive balancing among the cells.
- MOSFET block (ideal, switching): Models the ideal switching behavior of n-channel MOSFETs. When the gate-source voltage exceeds a predefined threshold, the MOSFET

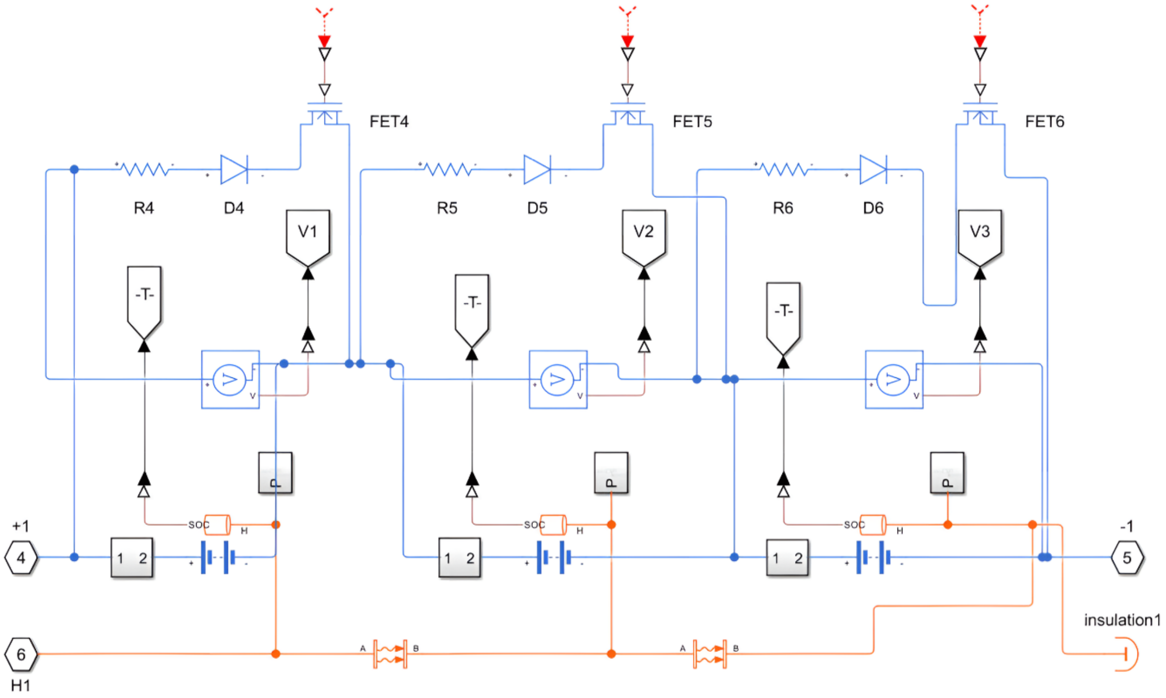

Figure 6. Three-cell series battery pack model

is activated, receiving signals from the passive balancing logic block to control its on/off state, thereby enabling passive balancing among the cells.

- Goto block: Facilitates data and signal transmission to corresponding receiving blocks within the model, ensuring communication among system components.

This model focuses on analyzing key battery pack parameters, including SOC, current (I), voltage (V), battery temperature, and the passive balancing process. Simulating a simplified battery pack reduces complexity and allows for a detailed analysis of critical factors affecting battery performance and durability in EV applications.

3.2. *Passive Balancing Logic Block Model*

This model takes the measured voltages of the cells as inputs, which are sent to tags V1, V2 and V3 (**Figure 7**). These voltages are processed through a transfer function to generate signals for the logic block. The outputs of the model are signals at ports s1, s2 and s3, which are transmitted to the MOSFET blocks described earlier. The logic block contains a Stateflow state diagram (**Figure 8**).

The passive voltage balancing block operates as follows: Initially, the logic values s1, s2, and s3 are set to 0. If the difference between the highest and lowest voltages among the three cells exceeds the allowable threshold (ΔV = 0.01 V) [22], the system initiates passive voltage balancing. The function sortV = ord(v_1, v_2, v_3) generates a matrix that sorts the voltage indices from lowest to highest, identifying the cell with the lowest voltage. If the first cell has the lowest voltage, the logic values s1 and s2 are set to 1 to activate the corresponding MOSFETs, thereby dissipating energy from the second and third cells to achieve passive balancing. During simulation, voltages are continuously measured and compared against the above conditions. If the first cell is no longer the one with the lowest voltage, the system resets s2 and s3 to 0 and applies the same logic to the other cells with the lowest voltage. When the voltage deviation among the cells falls below the allowable threshold, the balancing process terminates by setting all logic values s1, s2, and s3 to 0. This process ensures efficient voltage balancing among the cells, contributing to improved performance and longevity of the battery pack in EV applications.

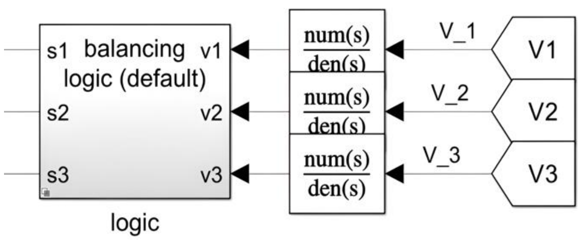

Figure 7. Passive balancing control logic model

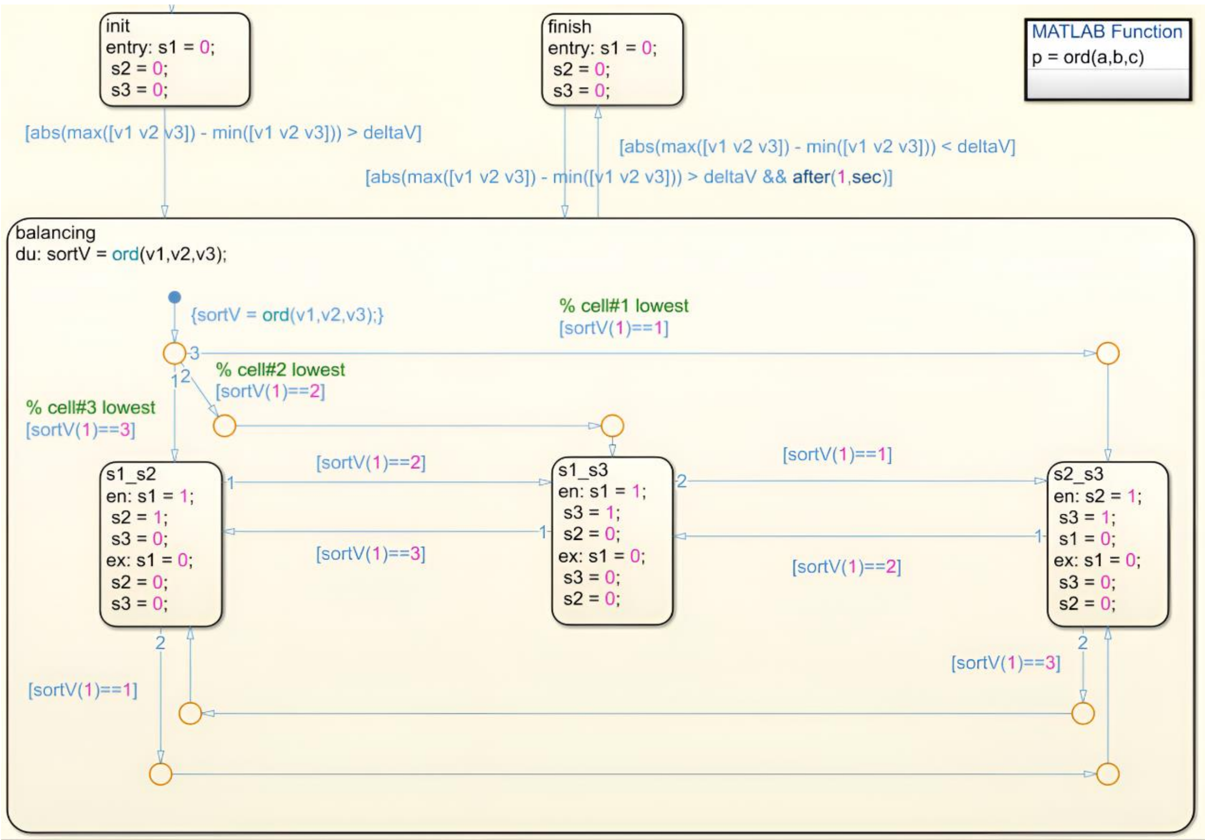

Figure 8. Passive balancing logic block state diagram

3.3. *Charge and Discharge Logic Model*

This block operates based on the highest SOC among the three cells (to prevent overcharging of the cell with the highest SOC) and the lowest SOC (to avoid over-discharging of the cell with the lowest SOC), generating logic for the charge-discharge process throughout the simulation as shown in **Figure 9** and **Figure 10**.

The charge and discharge logic block operates as follows (**Figure 11**):

If the highest SOC is less than 50%, the logic sets the tag mode to 1 to initiate charging. After charging, if the highest SOC exceeds 99% (indicating a full battery) or after 5,000 seconds (to simulate charge-discharge cycles for easier analysis of battery behavior if not fully charged), the system switches to discharge mode. The battery pack discharges until the lowest SOC falls below 30%, at which point the system reinitiates charging by setting the mode tag to 1.

If the highest SOC is initially above 50%, the system transitions to discharge mode by setting the mode tag to 2. The battery pack discharges until the lowest SOC falls below 30%, then switches back to charging by setting mode to 1.

After receiving charge or discharge signals from the mode tag, a switch is used to execute the charge-discharge process for the battery pack (**Figure 12**).

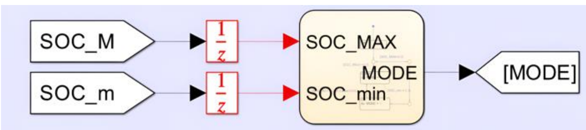

Figure 9. Charging and discharging logic block

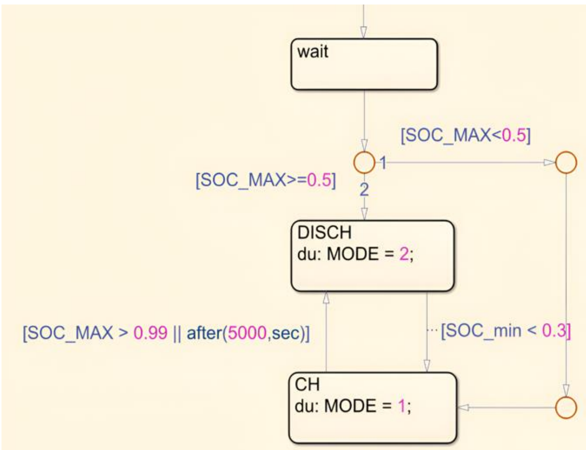

Figure 10. State diagram of the charge and discharge logic block

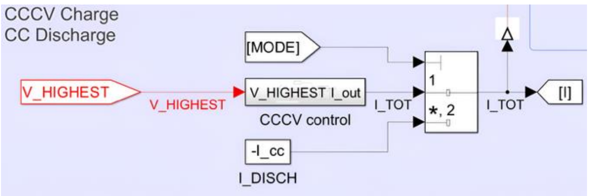

Figure 11. Charge and discharge control block model

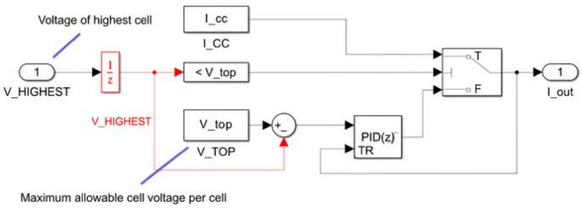

Figure 12. Charge current control block

Charging in the final stage, when the SOC of a cell is nearly full, is critical. Overcharging with excessive voltage at this stage can degrade battery quality and lifespan. Therefore, this block compares the voltage of the cell with the highest voltage to the maximum allowable voltage per cell, using a PID control block to reduce the charging voltage gradually.

3.4. *Simulation Model of the Three-Cell Series Battery Pack Operation*

This block is connected to voltage sensors, current sensors, and convective temperature sensors between the environment and the battery pack (**Figure 13**). To simulate the battery pack, it must be connected to a Solver Configuration block.

4. Simulation Results

4.1. *Simulated Battery Parameters*

The battery parameters used in the simulation are based on the specifications of Sanyo's Lithium-ion cells, model UR18650W (**Figure 14**). The technical specifications of the battery cell and ECM parameters are listed in **Table 1**.

4.2. *Simulation Results*

After setting up the parameters and running the simulation (**Figure 15**), it can be observed that the charging and discharging currents vary over time based on the duration and the charging state of the 3-cell series battery pack. During the charging phase, the current is positive, and the pack voltage increases. As the voltage approaches the maximum value (12.2 V), the current is gradually reduced to near zero to maintain voltage stability until the battery is fully charged. This approach prevents overcharging and avoids the dangers associated with rapid charging in the final stage, which could lead to overloading.

Table 1. Technical specifications of Sanyo UR18650W battery cells and ECM parameters (adapted from official datasheet [18], [20], [21]

Parameter		Value
Nominal capacity		1500 mAh
Nominal voltage		3.7 V
Charging method		Constant current, constant voltage
Charging voltage		4.2 V
Charging current		Std.1500 mA
Charging time		2.5 hours
Maximum weight		45.4 g
Maximum dimensions	Diameter (D)	18.10 mm
	Height (H)	64.80 mm
Energy density (Volume)		333Wh/l
Energy density (Weight)		122Wh/kg
Polarization resistance (R_1)		28,66 mΩ
Polarization capacitance (C_1)		1.17 F
Internal resistance (R_0)		46.11 mΩ
Operating temperature	Charge	0 °C ~ +40 °C
	Discharge	-20 °C ~ +60 °C
	Storage	-20 °C ~ +50 °C

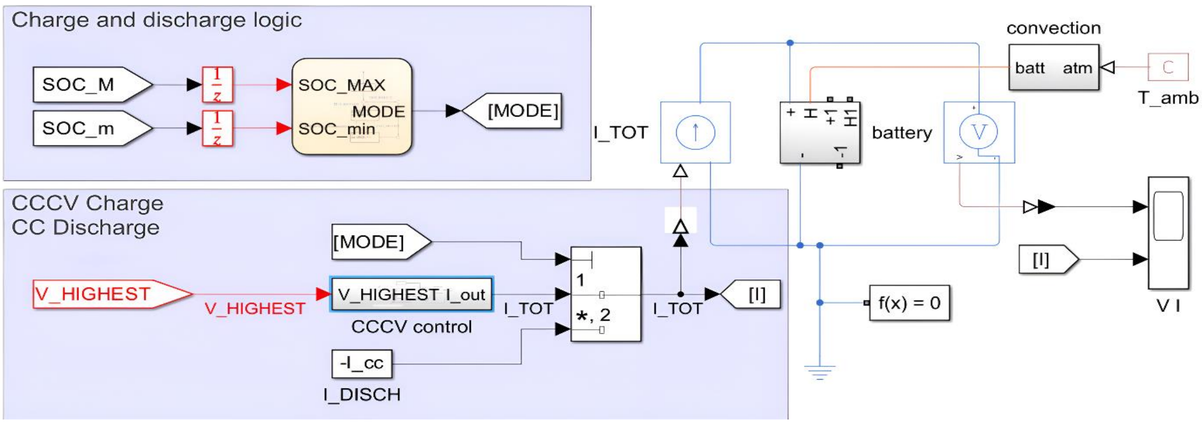

Figure 13. Complete simulation model

Figure 14. Sanyo UR18650W battery cells

Once the battery is nearly fully charged (99%), the discharge process begins with a constant current of 4 A. Discharging continues until the state of charge (SOC) drops below the set threshold of 30%, after which the charging process recommences. This charge-discharge cycle continues until the simulation time concludes. Overall pack voltage uniformity achieves std. dev. <0.005 V post-cycle 2 (97% improvement from pre-balancing 0.15 V), ensuring stable operation under urban EV loads

Figure 16 shows the voltage and current variations of each cell within the 3-cell series pack. Initially, the voltages of the individual cells differ due to the different SOC settings at the start of the simulation. However, after nearly one charge-discharge cycle, the voltage differences among the three cells become minimal, nearly negligible. This stabilization is achieved through passive balancing among the three cells. Voltage uniformity (std. dev.) reduces from 0.15 V (pre-balancing) to 0.005 V (post-cycle 2), a 97% improvement; current ripple remains <0.2 A across cells, validating MOSFET switching logic.

SOC trajectories for each cell illustrate initial variations (8.5% std. dev.), converging to near-equal levels by the second charging cycle through passive balancing, preventing underutilization and enhancing pack capacity (**Figure 17**). Without balancing, SOC mismatches would halt charging

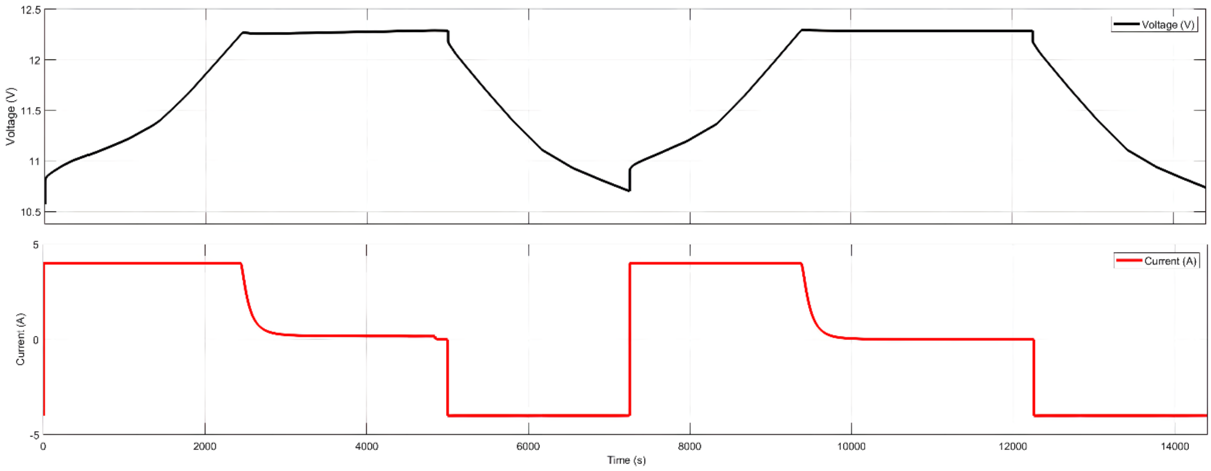

Figure 15. Voltage and current graph of the 3-cell series battery pack

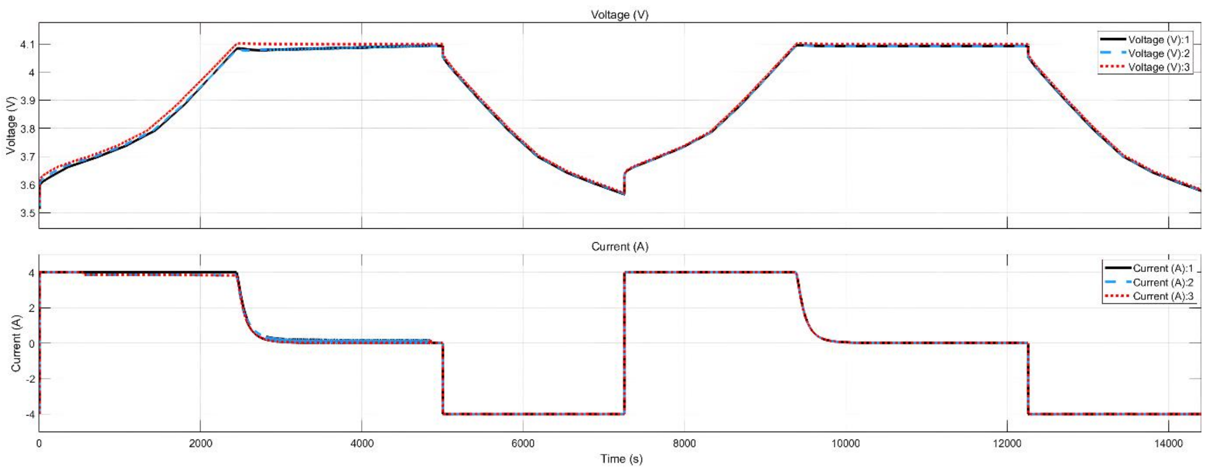

Figure 16. Voltage and current graph of each battery cell

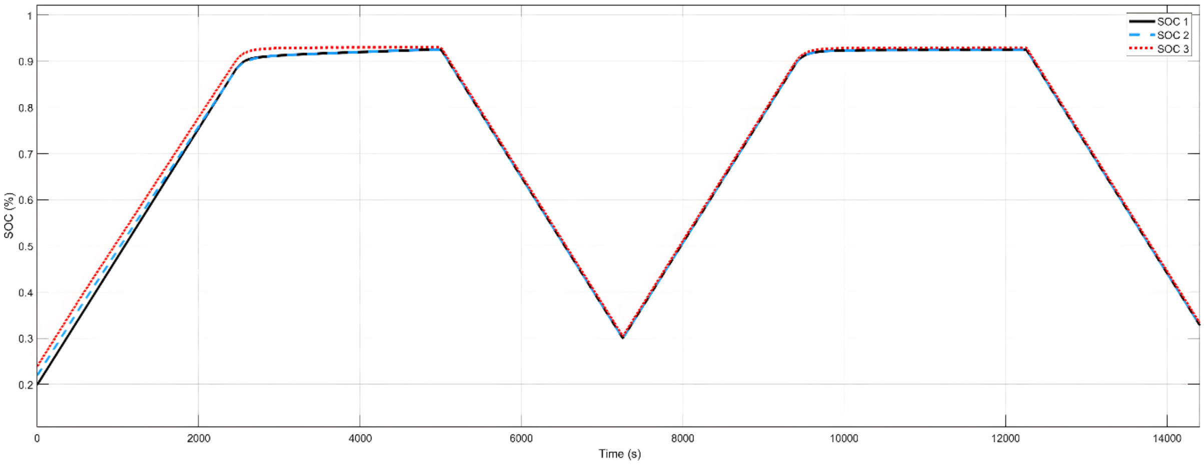

Figure 17. State of Charge (SOC) graph of the 3 battery cells

prematurely at ~99% for the leading cell. SOC std. dev. decreases from 8.5% (pre-balancing) to 0.8% (post-cycle 2), a 91% improvement; balancing time: 1.2 cycles to <1% deviation, enabling >95% effective capacity utilization. The SOC of Cell 1 reaches 99% at around 5,000 seconds, and the SOC difference between Cell 1 and Cell 3 reaches 8.5% at around 2,000 seconds, highlighting the need for effective balancing in real-world applications.

Temperature profiles during charge-discharge cycles reveal significant inter-cell differences due to positional effects (e.g., insulated central Cell 3) and balancing-induced dissipation (**Figure 18**). All cells remain within the safe 5–45°C range, with Cell 3 reaching a peak temperature of 40°C at around 10,000 seconds. The maximum ΔT rise is 2.5°C during peak discharge, with an overall max variance of 2.1°C post-balancing, representing a 50% improvement from the initial 4.2°C. This confirms thermal stability, with heat generation aligned to Eq. 6 (<1 W per cell at 4 A discharge). The temperature difference between Cell 1 and Cell 3 reaches 10°C at around 8,000 seconds, highlighting the need for effective thermal management in real-world applications.

5. Conclusion

The simulated 3-cell lithium-ion battery pack demonstrated partial passive balancing under idealized conditions. After one charge-discharge cycle, voltage differences between cells were reduced to <0.01 V, and SOC discrepancies were minimized by the second cycle. However, this result is limited to a small-scale configuration (3 cells) and may not fully represent real-world battery packs with hundreds of cells. While this optimization shows promise, further validation is needed for larger systems.

The simulation confirmed that the charging control algorithm effectively reduced current as voltage approached the 12.2 V threshold, preven-

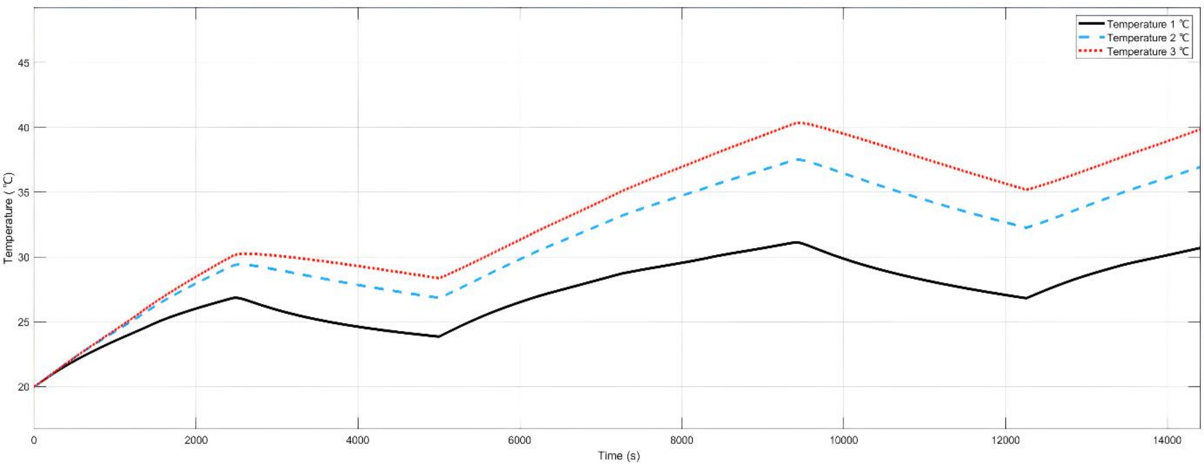

Figure 18. Temperature graph of the battery

ting overcharging. The discharge process maintained a stable 4 A until SOC dropped to 30%, at which point recharging was initiated. However, this performance was observed under controlled conditions (constant current, no load fluctuations), and real-world EV applications may require more adaptive control strategies.

The model showed minor temperature variations among cells, with the centrally insulated third cell exhibiting slightly higher temperatures. All cells remained within the 5–45 °C safe operating range, consistent with Sanyo UR18650W specifications. However, this result is based on an idealized thermal model and does not account for dynamic thermal gradients in larger battery packs or extreme environmental conditions.

While the simulation successfully demonstrated basic passive balancing, charging control, and temperature management in a small-scale 3-cell battery pack, these results are limited by the model's simplicity and idealized conditions. Further testing with larger packs, real-world load profiles, and more sophisticated thermal models is necessary before applying these findings to practical EV applications.

Author's Declaration

Authors' contributions and responsibilities

The authors made substantial contributions to the conception and design of the study. The authors took responsibility for data analysis, interpretation and discussion of results. The authors read and approved the final manuscript.

Funding

No funding information from the authors.

Availability of data and materials

All data are available from the authors.

Competing interests

The authors declare no competing interest.

Additional information

No additional information from the authors.

References

[1] N. K. Tuan, K. E. Karpukhin, A. S. Terenchenko, and A. F. Kolbasov, "World trends in the development of vehicles with alternative energy sources," *ARPN Journal of Engineering and Applied Sciences*, vol. 13, no. 7, pp. 2535–2542, 2018.

[2] M. A. Majid, C. R. K. J, and A. Ahmed, "Advances in electric vehicles for a self-reliant energy ecosystem and powering a sustainable future in India," *e-Prime - Advances in Electrical Engineering, Electronics and Energy*, vol. 10, p. 100753, Dec. 2024, doi: 10.1016/j.prime.2024.100753.

[3] V. H. Quan, N. T. Duc, and H. Q. Tuan, "Research and Simulation of Regenerative Braking System Using PMSM Motor with FOC Control Method Applying SVPWM Algorithm," *International Journal of Mechanical Engineering and Robotics Research*, vol. 14, no. 2, pp. 176–183, 2025, doi: 10.18178/ijmerr.14.2.176-183.

[4] K. R. Ngoy *et al.*, "Lithium-ion batteries and the future of sustainable energy: A comprehensive review," *Renewable and Sustainable Energy Reviews*, vol. 223, p. 115971, Nov. 2025, doi: 10.1016/j.rser.2025.115971.

[5] N. T. Duc, V. H. Quan, N. H. Minh, and K. E. Karpukhin, "Study on the analysis of the efficiency of the cooling system of the traction battery of an electric vehicle in a real cycle [In Russian]," *Proceedings of NAMI [In Russian]*, no. 1, 2025, doi: https://nami.elpub.ru/jour/article/view/368.

[6] A. Ashraf, B. Ali, M. S. A. Al Sunjury, and P. Tricoli, "A Comprehensive Review of the Art of Cell Balancing Techniques and Trade-Offs in Battery Management Systems," *Energies*, vol. 18, no. 13, p. 3321, Jun. 2025, doi: 10.3390/en18133321.

[7] J. Meng, G. Luo, M. Ricco, M. Swierczynski, D.-I. Stroe, and R. Teodorescu, "Overview of Lithium-Ion Battery Modeling Methods for State-of-Charge Estimation in Electrical Vehicles," *Applied Sciences*, vol. 8, no. 5, p. 659, Apr. 2018, doi: 10.3390/app8050659.

[8] Amin, K. Ismail, A. Nugroho, and S. Kaleg, "Passive balancing battery management system using MOSFET internal resistance as balancing resistor," in *2017 International Conference on Sustainable Energy Engineering and Application (ICSEEA)*, IEEE, Oct. 2017, pp. 151–155. doi: 10.1109/ICSEEA.2017.8267701.

[9] M. Uzair, G. Abbas, and S. Hosain, "Characteristics of Battery Management Systems of Electric Vehicles with Consideration of the Active and Passive Cell

Balancing Process," *World Electric Vehicle Journal*, vol. 12, no. 3, p. 120, Aug. 2021, doi: 10.3390/wevj12030120.

[10] X. Li and R. Setiowati, "The Influence of Country of Origin, Brand Awareness, Perceived Risk and Brand Image on Purchase Intention on China Wuling Air Electric Vehicles," *Open Journal of Applied Sciences*, vol. 13, no. 05, pp. 618–635, 2023, doi: 10.4236/ojapps.2023.135049.

[11] X. Yi, G. Qi, X. Liu, C. Depcik, and L. Liu, "Challenges and strategies toward anode materials with different lithium storage mechanisms for rechargeable lithium batteries," *Journal of Energy Storage*, vol. 95, p. 112480, Aug. 2024, doi: 10.1016/j.est.2024.112480.

[12] V. N. Kozlov, A. F. Kolbasov, K. E. Karpukhin, and N. T. Katanaev, "Mathematical model of an electric vehicle with a non-flat battery of photovoltaic converters," *IOP Conference Series: Materials Science and Engineering*, vol. 819, no. 1, p. 012014, Apr. 2020, doi: 10.1088/1757-899X/819/1/012014.

[13] D. Endachev *et al.*, "Hybrid Energy Storage on Electric Vehicles," in *Advances in Engineering Research and Application*, 2024, pp. 27–35. doi: 10.1007/978-3-031-62235-9_4.

[14] A. V. Klimov, B. K. Ospanbekov, A. V. Keller, S. S. Shadrin, D. A. Makarova, and Y. M. Furletov, "Research into the Peculiarities of the Individual Traction Drive Nonlinear System Oscillatory Processes," *World Electric Vehicle Journal*, vol. 14, no. 11, p. 316, Nov. 2023, doi: 10.3390/wevj14110316.

[15] V. Srinivasan, "Battery Pack Modeling and Performance Assessment for Electric Vehicle Applications," Chalmers University of Technology, 2021.

[16] N. D. Quang, "Comprehensive research and evaluation of electric vehicle batteries: Technology, models and simulations to calculate battery performance on GM EV1 [In Vietnam]," *Journal of Energy Science and Technology - University of Electricity*, vol. 1, 2024.

[17] S. Rao K and K. Vasudha, "The performance analysis of modified generic model for Lithium-ion batteries," *IOP Conference Series: Earth and Environmental Science*, vol. 1042, no. 1, p. 012011, Jul. 2022, doi: 10.1088/1755-1315/1042/1/012011.

[18] K. Saqli, H. Bouchareb, N. K. M'Sirdi, and M. O. Bentaie, "An overview of State of Charge (SOC) and State of Health (SOH) estimation methods of Li-ion batteries," in *Proceedings of the 12th International Conference on Integrated Modeling and Analysis in Applied Control and Automation (IMAACA 2019)*, 2019. doi: 10.46354/i3m.2019.imaaca.013.

[19] M. Berecibar, I. Gandiaga, I. Villarreal, N. Omar, J. Van Mierlo, and P. Van den Bossche, "Critical review of state of health estimation methods of Li-ion batteries for real applications," *Renewable and Sustainable Energy Reviews*, vol. 56, pp. 572–587, Apr. 2016, doi: 10.1016/j.rser.2015.11.042.

[20] H. Berg, *Batteries for Electric Vehicles*. Cambridge University Press, 2015. doi: 10.1017/CBO9781316090978.

[21] Y. Tan, Y. Li, Y. Gu, W. Liu, J. Fang, and C. Pan, "Numerical Study on Heat Generation Characteristics of Charge and Discharge Cycle of the Lithium-Ion Battery," *Energies*, vol. 17, no. 1, p. 178, Dec. 2023, doi: 10.3390/en17010178.

[22] P. C. John and B. P. N. Kumar, "Functional Safety Design and ISO26262 Compliance for BMS in EV and HEV," in *Intelligent Solutions for Smart Grids and Smart Cities*, 2023, pp. 329–339. doi: 10.1007/978-981-99-0915-5_23.